ASER Analysis of TAS/MRC System with HQAM under Generalized-K Fading Channels

Rajkishur Mudoi[1]

[1]Department of Electronics and Communication Engineering, North-Eastern Hill University, Shillong, Meghalaya, 793022, India

Email: rajkishur@gmail.com

Abstract: The average symbol error rate (ASER) of a multiple-input multiple-output (MIMO) system under generalized-K fading channels is analyzed in this work. The hexagonal quadrature amplitude modulation (HQAM) technique is applied to evaluate the ASER. Transmit antenna selection (TAS) at the base station is performed and maximal ratio combining (MRC) at the receiver is considered for the downlink transmission. Depending on the channel state information (CSI), the antenna at the transmit end that maximizes the MRC output SNR is selected for transmission. The effect of fading parameters on the ASER of the system has been investigated. The effect of the number of transmit and receive antennas on the system has been analyzed. The dependence of constellation size and the adjustment parameter on the ASER performance is examined.

Keywords: ASER, Generalized-K Distribution, TAS/MRC, MIMO, HQAM.

I. INTRODUCTION

In beyond 5G as well as 6G wireless communication systems very high data rates and energy efficiency can be achieved by the application of higher order two-dimensional (2D) constellations such as hexagonal quadrature amplitude modulation (HQAM). HQAM has the densest 2D packing, thereby providing reduced peak as well as average constellation power [1]. HQAM is utilized in multiple-antenna systems, optical communications, advanced channel coding and multicarrier systems [2].

The multiple-input-multiple-output (MIMO) is used to improve the channel throughput. For a large number of antennas, the hardware complexity as well as the price of the MIMO scheme goes high. Simultaneous transmissions from multiple antennas have the inherent disadvantages of inter-antenna interference, the requirement of synchronization etc. The transmit antenna selection (TAS) is one of the most useful technique to overcome these disadvantages. In the TAS scheme, the CSI of all links are sent back to the base station and based on CSI information the transmitter allots the best antenna for the transmission. The most useful diversity combining method is the maximal ratio combining (MRC), where the received SNR at all the receiving antennas are added to maximize the receiver output SNR. The TAS scheme has been investigated over various flat fading channels in the past. In [3], the expression of ABER for TAS/MRC communication systems under Hoyt fading channels has been examined and in [4] the derivation for both outage probability as well as exact SER for the TAS/MRC scheme has been presented.

In wireless communication, as a result of fading the received signals experience differences in attenuation, delay and phase shift. The generalized-K (K_G) distribution can be used to model the fading, shadowing and the propagation path-loss experienced in mobile communication channels [5]. K_G fading distribution is a composite fading that consists of Nakagami-*m* and Gamma distribution. The K_G fading model is a generalized model as it can be used to approximate other fading models, such as K fading, and Rayleigh-Lognormal (R-L) [5][6][7]. It can usually cover many transmission scenarios obtained in real wireless systems, than the other composite channel models [8]. In [6], the outage probability and the channel capacity over K_G fading channel are analyzed. However, the ASER analysis of specific wireless communication structures like TAS/MRC operating under the influence of K_G channels is not available in the technical literature. In this work, ASER performance with HQAM technique for the TAS at the base station and MRC at the receiver under K_G fading channel is investigated.

II. METHODOLOGY

The TAS/MRC wireless transmission system with T_A transmit antennas at the base station and R_A receive antennas with the user is depicted in Figure 1. Through the application of channel state information (CSI), the scheduler of the base station selects the best transmit antenna which maximizes the post-processing SNR at the output of the MRC receiver. The channel between the transmit antenna and the user is modelled as a slow flat K_G fading channel. MRC diversity is carried out by the user of the system to improve the quality of the downlink information. In the MRC receiver, the received signals from all diversity antennas are co-phased, multiplied by a weight factor proportional to the branch SNR and added together.

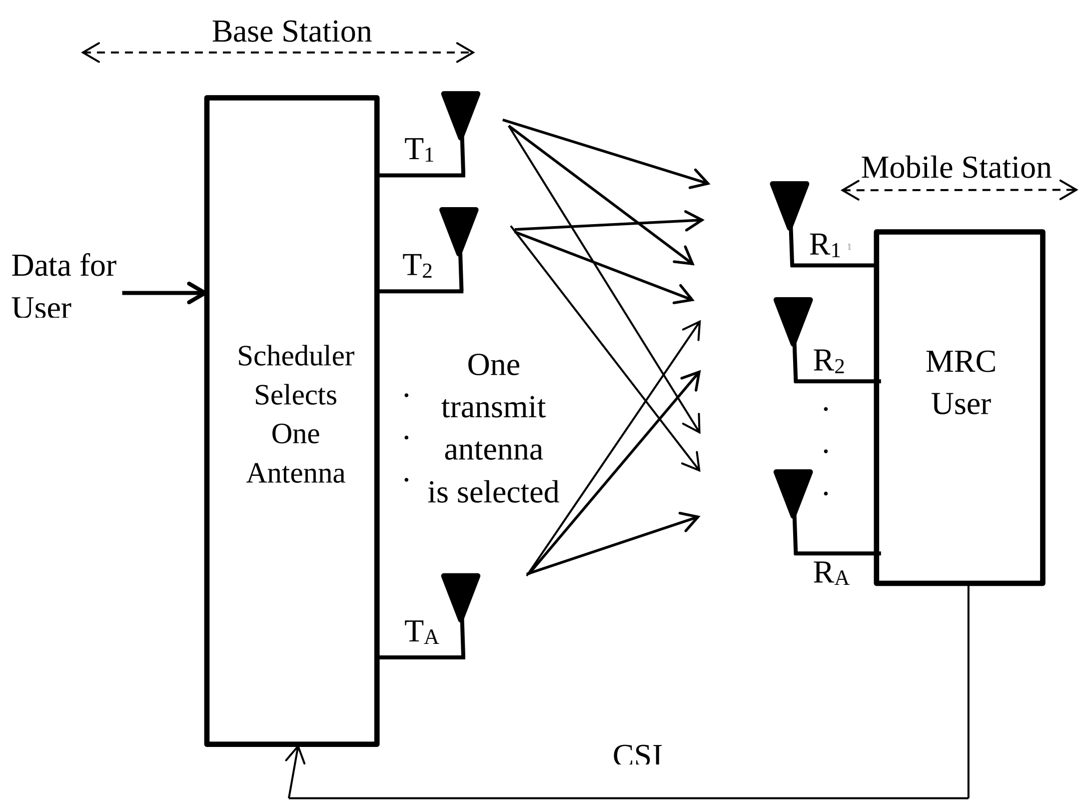

Figure1: TAS with MRC receiver system

It was verified that both a single K_G RV and the sum of independent K_G RVs can be approximated by a single Gamma RV [9]. Denoting γ_i as a Gamma distributed RV with a shape parameter ρ and a scale parameter θ, the probability density function (PDF) of the instantaneous SNR γ_i is given as [10][11]

$$f_{\gamma_i}(\gamma) = \frac{\theta^{-\rho}}{\Gamma(\rho)} \gamma^{\rho-1} \exp\left(-\frac{\gamma}{\theta}\right). \tag{1}$$

Whereby, $\Gamma(\cdot)$ is the Gamma function; $\theta = (AF - \varepsilon)\bar{\gamma}$ and $\rho = \frac{R_A}{AF - \varepsilon}$. The AF represents the amount of fading and $AF = \frac{1}{m} + \frac{1}{k} + \frac{1}{mk}$. Moreover, ε is the adjustment parameter. m and k are the fading parameters. The CDF of the instantaneous SNR over a K_G fading channel is expressed as

$$F_{\gamma_i}(\gamma) = \frac{\theta^{-\rho}}{\Gamma(\rho)} \int_0^{\gamma} \gamma^{\rho-1} \exp\left(-\frac{\gamma}{\theta}\right) d\gamma. \tag{2}$$

Simplifying by utilizing [12, (3.381.1)],

$$F_{\gamma_i}(\gamma) = \left[\frac{1}{\Gamma(\rho)} g\left(\rho, \frac{\gamma}{\theta}\right)\right], \tag{3}$$

whereby, $g(.,.)$ is the lower incomplete Gamma function. In TAS with MRC at the receiver system, the best γ is selected from $T_A R_A$ number of RVs. The CDF of which can be written as

$$F_{\gamma}(\gamma) = \frac{1}{\left[\Gamma(\rho)\right]^{T_A}} \left[g\left(\rho, \frac{\gamma}{\theta}\right)\right]^{T_A}. \tag{4}$$

Therefore, the PDF of the output SNR is

$$f_{\gamma}(\gamma) = \frac{T_A}{\left[\Gamma(\rho)\right]^{T_A}} \left[g\left(\rho, \frac{\gamma}{\theta}\right)\right]^{T_A - 1} \frac{d}{d\gamma}\left[g\left(\rho, \frac{\gamma}{\theta}\right)\right]. \tag{5}$$

Differentiating the lower incomplete Gamma function with the help of [13, (6.5.25)],

$$f_{\gamma}(\gamma) = \frac{T_A}{\theta^{\rho}\left[\Gamma(\rho)\right]^{T_A}} \left[g\left(\rho, \frac{\gamma}{\theta}\right)\right]^{T_A - 1} \gamma^{\rho-1} e^{-\frac{\gamma}{\theta}}. \tag{6}$$

Writing the $g(.,.)$ in infinite series applying [14, (1.7)], the pdf of output SNR for TAS/MRC system over K_G fading channel is derived as

$$f_\gamma(\gamma)=\frac{T_A}{\left[\Gamma(\rho)\right]^{T_A}}\sum_{n_1=0}^{\infty}\sum_{n_2=0}^{\infty}\cdots\sum_{n_{T_A-1}=0}^{\infty}\frac{\left(\frac{1}{\theta}\right)^{T_A\rho+\sum_{i=1}^{T_A-1}n_i}}{\prod_{i=1}^{T_A-1}(\rho)_{n_i+1}}\left(e^{-T_A\frac{\gamma}{\theta}}\right)\gamma^{\left(T_A\rho+\sum_{i=1}^{T_A-1}n_i\right)-1}. \tag{7}$$

III. ASER ANALYSIS

The ASER depends on the fading distribution and modulation technique. It can be given as [15],

$$P_e=\int_0^\infty p(e|\gamma)\,f_\gamma(\gamma)d\gamma\,, \tag{8}$$

where, $p(e|\gamma)$ is the conditional error probability. For *M*-ary HQAM, the $p(e|\gamma)$ is expressed as [16] [17],

$$p(e|\gamma)=V_{ZZ}Q\left(\sqrt{\varphi\gamma}\right)+\frac{2}{3}V_{ZZ}Q^2\left(\sqrt{\frac{2\varphi\gamma}{3}}\right)-2V_{WZZ}Q\left(\sqrt{\varphi\gamma}\right)Q\left(\sqrt{\frac{\varphi\gamma}{3}}\right). \tag{9}$$

whereby, $\varphi=\frac{24}{7M-4}, V_{ZZ}=2\left(3-\frac{4}{\sqrt{M}}+\frac{1}{M}\right)$, as well as $V_{WZZ}=6\left(1-\frac{1}{\sqrt{M}}\right)^2$. Prony approximation may be applied for the Gaussian *Q*-function $Q(.)$. Prony approximation with two exponential terms can be obtained as $Q(\lambda)\approx\partial e^{-t\lambda^2}+\tau e^{-u\lambda^2}$ [18]. The value of the constants are $\partial=0.208$, $\tau=0.147$, $t=0.971$, and $u=0.525$. Putting the value of $f_\gamma(\gamma)$ and $p(e|\gamma)$ into (8), the ASER can be given as

$$P_e=\Delta_1+\Delta_2-\Delta_3\,. \tag{10}$$

Where,

$$\Delta_1=V_{ZZ}\frac{T_A}{\left[\Gamma(\rho)\right]^{T_A}}\sum_{n_1=0}^{\infty}\sum_{n_2=0}^{\infty}\cdots\sum_{n_{T_A-1}=0}^{\infty}\frac{\left(\frac{1}{\theta}\right)^{T_A\rho+\sum_{i=1}^{T_A-1}n_i}}{\prod_{i=1}^{T_A-1}(\rho)_{n_i+1}}\left[\int_0^\infty\partial e^{-\gamma\left(t\varphi+\frac{T_A}{\theta}\right)}\gamma^{\left(T_A\rho+\sum_{i=1}^{T_A-1}n_i\right)-1}d\gamma\right.$$
$$\left.+\int_0^\infty\tau e^{-\gamma\left(u\varphi+\frac{T_A}{\theta}\right)}\gamma^{\left(T_A\rho+\sum_{i=1}^{T_A-1}n_i\right)-1}d\gamma\right]. \tag{11}$$

$$\Delta_2 = \frac{2}{3} V_{ZZ} \frac{T_A}{\left[\Gamma(\rho)\right]^{T_A}} \sum_{n_1=0}^{\infty} \sum_{n_2=0}^{\infty} \cdots \sum_{n_{T_A-1}=0}^{\infty} \frac{\left(\frac{1}{\theta}\right)^{T_A\rho + \sum_{i=1}^{T_A-1} n_i}}{\prod_{i=1}^{T_A-1} (\rho)_{n_i+1}} \left[\int_0^{\infty} \partial^2 e^{-\gamma\left(\frac{4t\varphi}{3} + \frac{T_A}{\theta}\right)} \gamma^{\left(T_A\rho + \sum_{i=1}^{TA-1} n_i\right)-1} d\gamma \right.$$

$$\left. + \int_0^{\infty} 2\partial\tau e^{-\gamma\left\{\left(\frac{2t\varphi}{3} + \frac{2u\varphi}{3}\right) + \frac{T_A}{\theta}\right\}} \gamma^{\left(T_A\rho + \sum_{i=1}^{T_A-1} n_i\right)-1} d\gamma + \int_0^{\infty} \tau^2 e^{-\gamma\left(\frac{4u\varphi}{3} + \frac{T_A}{\theta}\right)} \gamma^{\left(T_A\rho + \sum_{i=1}^{T_A-1} n_i\right)-1} d\gamma \right]. \quad (12)$$

And,

$$\Delta_3 = 2V_{WZZ} \frac{T_A}{\left[\Gamma(\rho)\right]^{T_A}} \sum_{n_1=0}^{\infty} \sum_{n_2=0}^{\infty} \cdots \sum_{n_{T_A-1}=0}^{\infty} \frac{\left(\frac{1}{\theta}\right)^{T_A\rho + \sum_{i=1}^{T_A-1} n_i}}{\prod_{i=1}^{T_A-1} (\rho)_{n_i+1}} \left[\int_0^{\infty} \partial^2 e^{-\gamma\left(\frac{4t\varphi}{3} + \frac{T_A}{\theta}\right)} \gamma^{\left(T_A\rho + \sum_{i=1}^{T_A-1} n_i\right)-1} d\gamma \right.$$

$$+ \int_0^{\infty} \partial\tau e^{-\gamma\left\{\left(t\varphi + u\frac{\varphi}{3}\right) + \frac{T_A}{\theta}\right\}} \gamma^{\left(T_A\rho + \sum_{i=1}^{T_A-1} n_i\right)-1} d\gamma + \int_0^{\infty} \partial\tau e^{-\gamma\left\{\left(u\varphi + t\frac{\varphi}{3}\right) + \frac{T_A}{\theta}\right\}} \gamma^{\left(T_A\rho + \sum_{i=1}^{T_A-1} n_i\right)-1} d\gamma$$

$$\left. + \int_0^{\infty} \tau^2 e^{-\gamma\left(\frac{4u\varphi}{3} + \frac{T_A}{\theta}\right)} \gamma^{\left(T_A\rho + \sum_{i=1}^{T_A-1} n_i\right)-1} d\gamma \right]. \quad (13)$$

Solving the integrals using [12, (3.381.4)],

$$\Delta_1 = V_{ZZ} \frac{T_A}{\left[\Gamma(\rho)\right]^{T_A}} \sum_{n_1=0}^{\infty} \sum_{n_2=0}^{\infty} \cdots \sum_{n_{T_A-1}=0}^{\infty} \frac{\left(\frac{1}{\theta}\right)^{T_A\rho + \sum_{i=1}^{T_A-1} n_i} \Gamma\left(T_A\rho + \sum_{i=1}^{T_A-1} n_i\right)}{\prod_{i=1}^{T_A-1} (\rho)_{n_i+1}}$$

$$\times \left\{ \frac{\partial}{\left(t\varphi + \frac{T_A}{\theta}\right)^{\left(T_A\rho + \sum_{i=1}^{T_A-1} n_i\right)}} + \frac{\tau}{\left(u\varphi + \frac{T_A}{\theta}\right)^{\left(T_A\rho + \sum_{i=1}^{T_A-1} n_i\right)}} \right\}. \quad (14)$$

$$\Delta_2 = \frac{2}{3} V_{ZZ} \frac{T_A}{\left[\Gamma(\rho)\right]^{T_A}} \sum_{n_1=0}^{\infty} \sum_{n_2=0}^{\infty} \cdots \sum_{n_{T_A-1}=0}^{\infty} \frac{\left(\frac{1}{\theta}\right)^{T_A\rho + \sum_{i=1}^{T_A-1} n_i} \Gamma\left(T_A\rho + \sum_{i=1}^{T_A-1} n_i\right)}{\prod_{i=1}^{T_A-1} (\rho)_{n_i+1}}$$

$$\times \left[\frac{\partial^2}{\left(\frac{4t\varphi}{3} + \frac{T_A}{\theta}\right)^{\left(T_A\rho + \sum_{i=1}^{T_A-1} n_i\right)}} + \frac{2\partial\tau}{\left\{\left(\frac{2t\varphi}{3} + \frac{2u\varphi}{3}\right) + \frac{T_A}{\theta}\right\}^{\left(T_A\rho + \sum_{i=1}^{T_A-1} n_i\right)}} + \frac{\tau^2}{\left(\frac{4u\varphi}{3} + \frac{T_A}{\theta}\right)^{\left(T_A\rho + \sum_{i=1}^{T_A-1} n_i\right)}} \right]. \quad (15)$$

And,

$$\Delta_3 = 2V_{WZZ} \frac{T_A}{\left[\Gamma(\rho)\right]^{T_A}} \sum_{n_1=0}^{\infty} \sum_{n_2=0}^{\infty} \cdots \sum_{n_{T_A-1}=0}^{\infty} \frac{\left(\frac{1}{\theta}\right)^{T_A\rho + \sum_{i=1}^{T_A-1} n_i} \Gamma\left(T_A\rho + \sum_{i=1}^{T_A-1} n_i\right)}{\prod_{i=1}^{T_A-1} (\rho)_{n_i+1}} \left[\frac{\partial^2}{\left(\frac{4t\varphi}{3} + \frac{T_A}{\theta}\right)^{\left(T_A\rho + \sum_{i=1}^{T_A-1} n_i\right)}} \right.$$

$$\left. + \frac{\partial\tau}{\left\{\left(t\varphi + u\frac{\varphi}{3}\right) + \frac{T_A}{\theta}\right\}^{\left(T_A\rho + \sum_{i=1}^{T_A-1} n_i\right)}} + \frac{\partial\tau}{\left\{\left(u\varphi + t\frac{\varphi}{3}\right) + \frac{T_A}{\theta}\right\}^{\left(T_A\rho + \sum_{i=1}^{T_A-1} n_i\right)}} + \frac{\tau^2}{\left(\frac{4u\varphi}{3} + \frac{T_A}{\theta}\right)^{\left(T_A\rho + \sum_{i=1}^{T_A-1} n_i\right)}} \right]. \quad (16)$$

IV. NUMERICAL RESULTS AND DELIBERATIONS

Numerically evaluated data for ASER with HQAM technique have been presented in this section. ASER vs. average SNR per branch (in dB), has been plotted in Figure 2, considering $T_A = 2$ and $R_A = 2$. From Figure 2, it is observed that for a fixed value of *k*, the ASER performance improves as the value of *m* increases, corresponding that the channel fading becomes less severe. Similarly, it has been observed that for a fixed value of *m* the ASER performance improves as the value of k increases, implying that the channel becomes less shadowing. The performance of the system gets better with the increase of the fading parameters. It is considered that the adjustment parameter $\varepsilon = 1$. Similarly, with the increase in the constellation size, the ASER performance deteriorates, since the more number of transmitted symbols are influenced by channel fading.

In Figure 3, the ASER is plotted against average SNR with different constellation sizes and fading parameters. For analysis $T_A = 3$ and $R_A = 2$ are kept constant. It is considered that $\varepsilon = 1$. The ASER performance improves with the increase in average SNR. From Figure 3, it is observed that ASER performance improves with the increase in the fading parameters as well as the decrease in the constellation size.

In Figure 4, ASER vs. Average SNR per branch $\bar{\gamma}$ (in dB), has been plotted for the HQAM scheme with different numbers of T_A and R_A. The fading parameters are kept constant at $k = 1, m = 1$. Again in the figure $M = 16$, and $\varepsilon = 1$. From Figure 4, one can observe that when the number of transmit antennas become larger for a fixed number of receive antennas, the ASER performance of the system improves. Similarly, the same observations can be made by increasing the number of receive antennas for a fixed number of transmit antennas. From the figure, it is observed that with the increase in selection gain, the ASER performance of the TAS with the MRC receiver system has improved.

In Figure 5, the ASER performance of TAS configuration with HQAM modulation and for different numbers of transmit antennas (T_A) and adjustment parameters (ε) is shown. In Figure 5, $k = 1$, $m = 2$, $M = 16$, and $R_A = 4$. One can observe that when the number of transmit antennas increase for a fixed number of receive antennas, the ASER performance of the system improves. From Figure 5, it is observed that with the increase in adjustment parameters (ε), the ASER performance of the system improves.

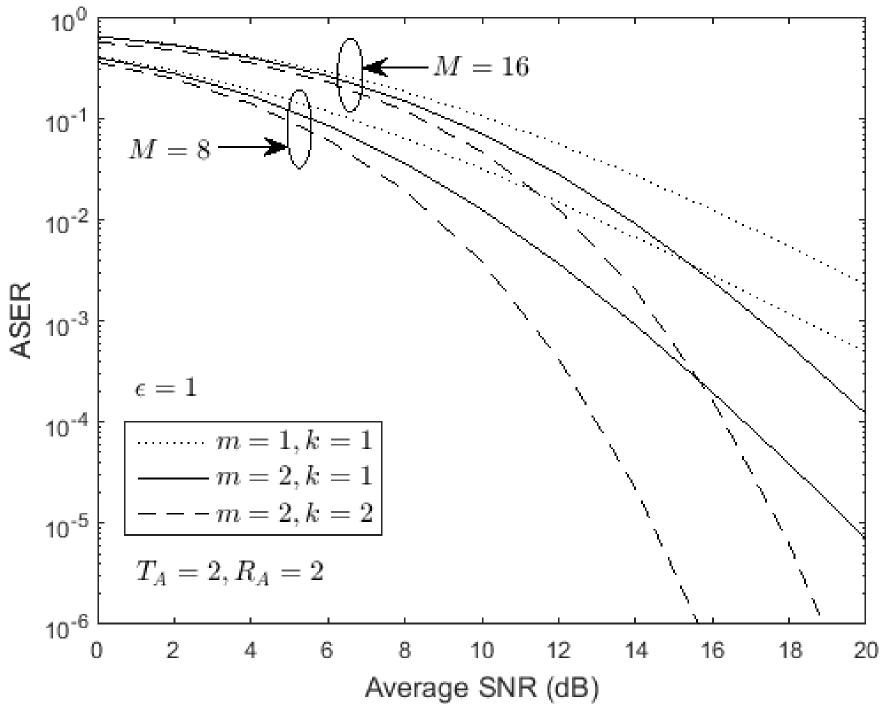

Figure 2: ASER vs. Average SNR in dB for different values of fading parameters and *M* with $T_A = 2, R_A = 2, \varepsilon = 1$.

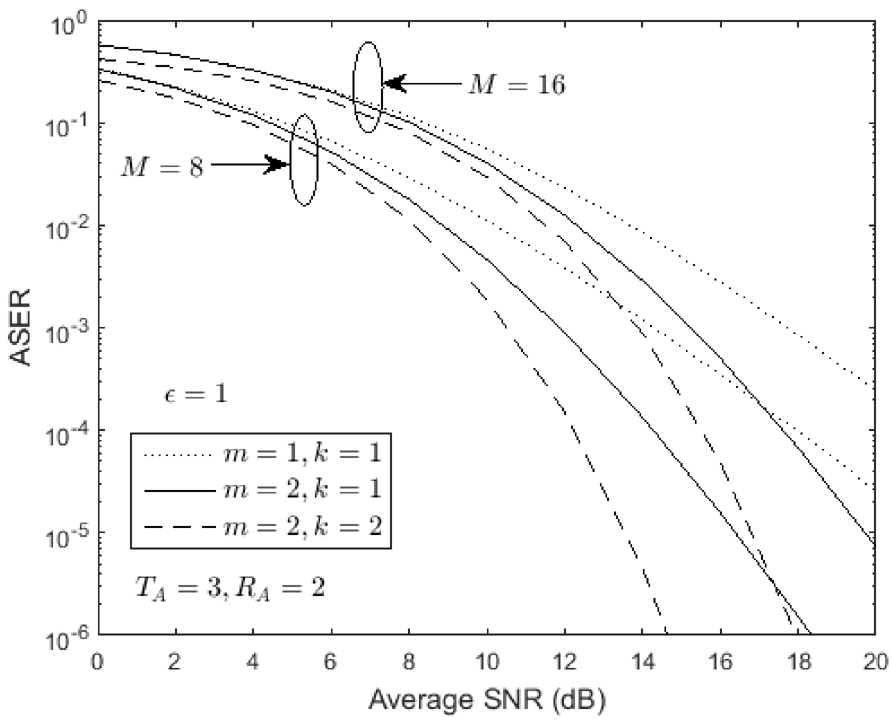

Figure 3: ASER vs. Average SNR in dB for different values of fading parameters and *M* with $T_A = 3, R_A = 2, \varepsilon = 1$.

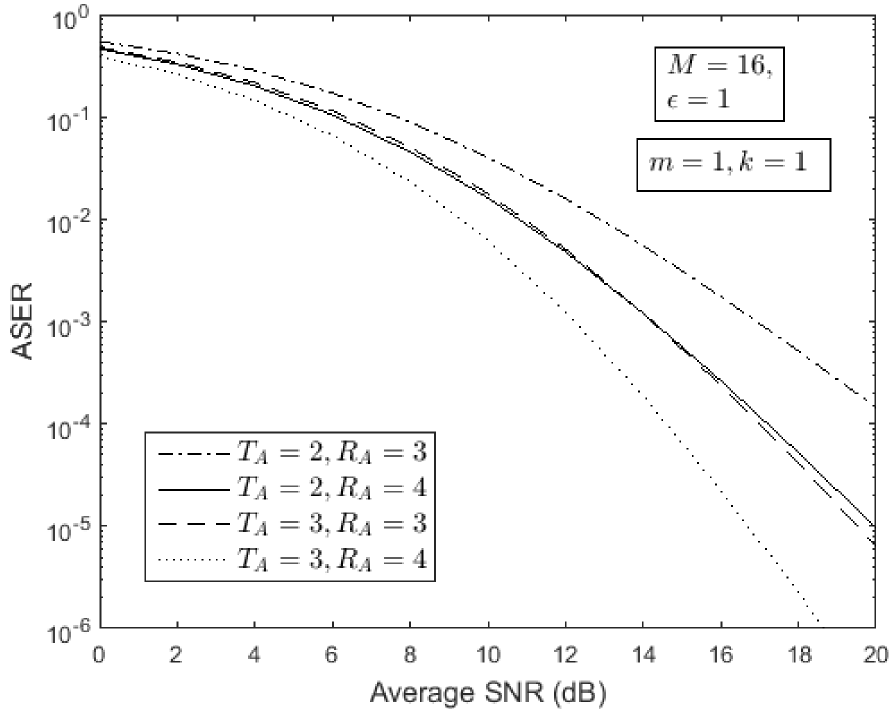

Figure 4: ASER vs. Average SNR (dB) for different numbers of transmit antennas (T_A) and received antennas (R_A) with $k = 1, m = 1$, $M = 16, \varepsilon = 1$.

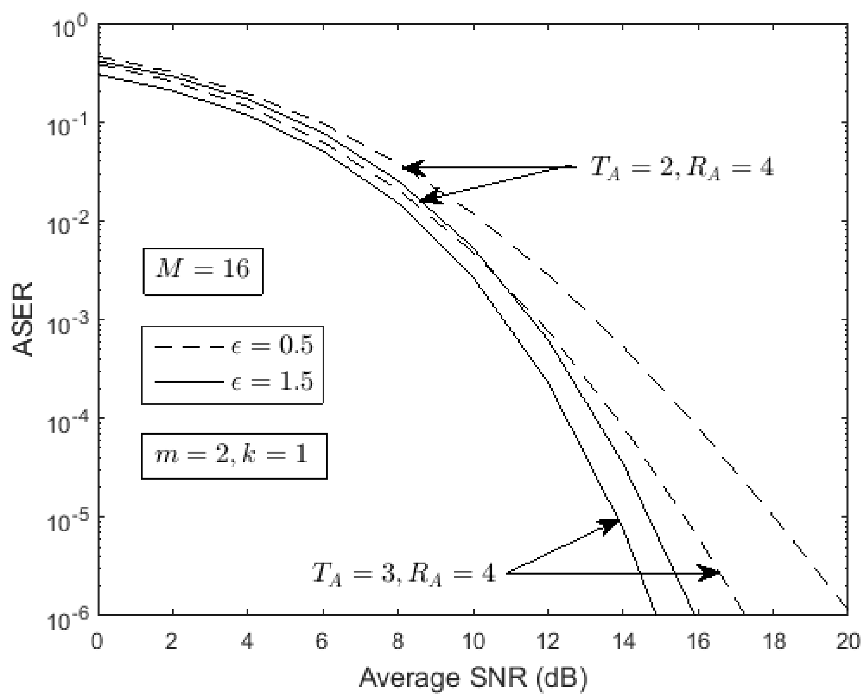

Figure 5: ASER vs. Average SNR (dB) for different number of transmit antennas (T_A) and adjustment parameters (ε) with $k = 1, m = 2$, $M = 16, R_A = 4$.

V. CONCLUSIONS

The ASER with HQAM over the K_G fading channels has been investigated. In this work, the TAS at the base station and MRC receiver scenario is considered. The expressions of the ASER have also been derived in terms of the Gamma function. The arbitrary number of transmit, receive antennas, fading parameters and adjustment parameter are considered for the analysis. Constellation size is varied from M=8 to M=16.

REFERENCES

[1] Thrassos K. Oikonomou, Sotiris A. Tegos, Dimitrios Tyrovolas, Panagiotis D. Diamantoulakis, and George K. Karagiannidis (2022), "On the Error Analysis of Hexagonal-QAM Constellations," IEEE Communications Letters, Vol. 26, No. 8, pp. 1764-1768.

[2] L. Rugini (2016), "Symbol error probability of hexagonal QAM," IEEE Communications Letters, Vol. 20, No. 8, pp. 1523–1526.

[3] Juan P. Pena-Martin, Juan M. Romero-Jerez, and Concepcion Tellez-Labao (2013), "Performance of TAS/MRC Wireless Systems under Hoyt Fading Channels," IEEE transactions on wireless communications, Vol.12, No. 7. pp. 3350-3359.

[4] Zhuo Chen, Jinhong Yuan and Branka Vucetic (2005), "Analysis of Transmit Antenna Selection/Maximal-Ratio Combining in Rayleigh Fading Channels," IEEE Transactions on Vehicular Technology, Vol. 54, No. 4, pp. 1312-1321.

[5] P. M. Shankar (2004), "Error rates in generalized shadowed fading channels", Wireless Personal Communications, Vol. 28, No. 4, pp. 233–238.

[6] Petros S. Bithas, Nikos C. Sagias, P. Takis Mathiopoulos, George K. Karagiannidis, and Athanasios A. Rontogiannis (2006), "On the Performance Analysis of Digital Communication over Generalized-k Fading Channel," IEEE Communications Letters, Vol. 10, No. 5, pp 353-355.

[7] A. Abdi and M. Kaveh (1998), "*K* distribution: An appropriate substitute for Rayleigh-lognormal distribution in fading-shadowing wireless channels," Electronics Letters, Vol. 34, No. 9, pp. 851–852.

[8] Jianfei Cao, Lie-Liang Yang and Zhangdui Zhong (2010), "Performance of Multihop Wireless Links over Generalized-*K* Fading Channel", IEEE 72nd Vehicular Technology Conference-Fall, Ottawa, ON, Canada.

[9] Saad Al-Ahmadi and Halim Yanikomeroglu (2010), "On the Approximation of the Generalized-K Distribution by a Gamma Distribution for Modeling Composite Fading Channels", IEEE Transactions on Wireless Communications, Vol. 9, No. 2, pp. 706-713.

[10] Rajkishur Mudoi and Chandana Brahma (2019), "Performance Analysis of Transmit Antenna Selection with Maximal Ratio Combining MIMO System Over Generalized-K Fading Channels," The IUP Journal of Electrical & Electronics Engineering, Vol. XII, No. 3, pp. 45-55.

[11] Hong-jiang Lei, Imran Shafique Ansai, Chao Gao, Yong-cai Guo, Gao-feng Pan, and Khalid A. Qaraqe (2016), "Secrecy performance analysis of single-input multiple-output generalized-K fading channels," Frontiers of Information Technology & Electronic Engineering, Vol. 17, No. 10, pp.1074-1084.

[12] I. S. Gradshteyn and I. M. Ryzhik (2000), Table of Integrals, Series and Products, 6th ed., San Diego, CA:Academic.

[13] M. Abramowitz and I. A. Stegun (1970), Handbook of Mathematical Functions, National Bureau of Standards.

[14] N. M. Temme (1994), "Computational Aspects of Incomplete Gamma Functions with Large Complex Parameters", International Series of Numerical Mathematics, Vol. 119, pp. 551-562.

[15] J. G. Proakis, Digital Communications, 4th Edition, McGraw-Hill, 2001.

[16] Luca Rugini, "Symbol error probability of hexagonal QAM," IEEE Communications Letters, vol. 20, no. 8, pp. 1523–1526, Aug. 2016.

[17] Dharmendra Sadhwani, "Simple and tightly approximated integrals over κ-μ shadowed fading channel with applications," IEEE Transactions On Vehicular Technology, vol. 67, no. 10, pp. 10092-10096, October 2018.

[18] Pavel Loskot, and Norman C. Beaulieu, "Prony and Polynomial approximations for evaluation of the average probability of error over slow-fading channels," IEEE Transactions on Vehicular Technology, vol. 58, no. 3, pp. 1269-1280, March 2009.